RESEARCH ARTICLE

Factors that Restrict the Cell Permeation of Cyclic Prodrugs of an Opioid Peptide, Part 3: Synthesis of Analogs Designed to Have Improved Stability to Oxidative Metabolism

REBECCA NOFSINGER, TARRA FUCHS-KNOTTS, RONALD T. BORCHARDT

Department of Pharmaceutical Chemistry, The University of Kansas, Lawrence, Kansas 66047

Received 26 March 2011; accepted 17 February 2012

Published online in Wiley Online Library (wileyonlinelibrary.com). DOI 10.1002/jps.23109

ABSTRACT: Previously, our laboratory reported that cyclic peptide prodrugs of the opioid peptide H-Tyr–D-Ala–Gly–Phe–D-Leu–OH (DADLE) are metabolized by cytochrome P450 (CYP450) enzymes, which limits their systemic exposure after oral dosing to animals. In an attempt to design more metabolically stable cyclic prodrugs of DADLE, we synthesized analogs of DADLE cyclized with a coumarinic acid linker (CA; CA–DADLE), which contained modifications in the amino acid residues known to be susceptible to CYP450 oxidation. Metabolic stability and metabolite identification studies of CA–DADLE and its analogs were then compared using rat liver microsomes (RLM), guinea pig liver microsomes (GPLM), and human liver microsomes (HLM), as well as recombinant human recombinant cytochrome P450 3A4 (hCYP3A4). Similar to the results observed for CA–DADLE, incubation of its analogs with RLM, GPLM, and HLM resulted in monohydroxylation of an amino acid side chain on these cyclic prodrugs. When CA–DADLE was incubated with hCYP3A4, similar oxidative metabolism of the peptide was observed. In contrast, incubation of the CA–DADLE analogs with hCYP3A4 showed that these amino-acid-modified analogs are not substrates for this CYP450 isozyme. These results suggest that the amino-acid-modified analogs of CA–DADLE prepared in this study could be stable to metabolic oxidation by CYP3A4 expressed in human intestinal mucosal cells. © 2012 Wiley Periodicals, Inc. and the American Pharmacists Association J Pharm Sci

Keywords: cyclic peptide prodrug; DADLE; opioid peptide; peptides; metabolism; cytochrome P450; oxidation; structure; synthesis

INTRODUCTION

Peptides and peptidomimetics have long been of interest to medicinal chemists and pharmacologists because of their intrinsic receptor specificity and promising pharmacological properties.[1–5] The preclinical and clinical development of these peptides and peptidomimetics has been limited by their undesirable biopharmaceutical properties, including poor intestinal mucosa permeation and enzymatic instability, which limits the blood levels observed after oral dosing.[6–9] A major challenge in making these chemotypes orally bioavailable lies in improving the biopharmaceutical properties of the peptides and peptidomimetics while maintaining their high affinity for their pharmacological receptors. For example, H-Tyr–D-Ala–Gly–Phe–D-Leu—OH (DADLE) was developed as a biologically active opioid peptide that is resistant to peptidase.[10,11] However, this opioid peptide exhibits poor permeation across biological barriers such as the blood–brain barrier and intestinal mucosa.[9,12–16]

In an attempt to improve the membrane permeability of opioid peptides, we have developed a

Abbreviations used: ACN, acetonitrile; Boc, *t*-butoxy carbonyl; CA, coumarinic acid linker; $CDCl_3$, chloroform-D; CH_2Cl_2, dichloromethane; DMAP, 4-dimethylamino pyridine; EDC-HCl, 1-(3-dimethylaminopropyl)-3-ethylcarbodiimide hydrochloride; GPLM, guinea pig liver microsomes; hCYP3A4, human recombinant cytochrome P450 3A4; HLM, human liver microsomes; HOBt, 1-hydroxybenzotriazole; MeOD, methanol-D4; $MgSO_4$, magnesium sulfate; $NHCO_3$, sodium bicarbonate; OAll, allyl protecting group; P-gp, P-glycoprotein; RLM, rat liver microsomes; TEA, triethyl amine; THF, terahydrofuran.

Correspondence to: Rebecca Nofsinger (Telephone: +215-652-4864; Fax: +215-616-6082; E-mail: Rebecca_Nofsinger@Merck.com)

Rebecca Nofsinger's present addresses is Merck & Company, West Point, Pennsylvania 19486.

Tarra Fuchs-Knotts's present addresses is Achaogen, South San Francisco, California 94080.

Journal of Pharmaceutical Sciences

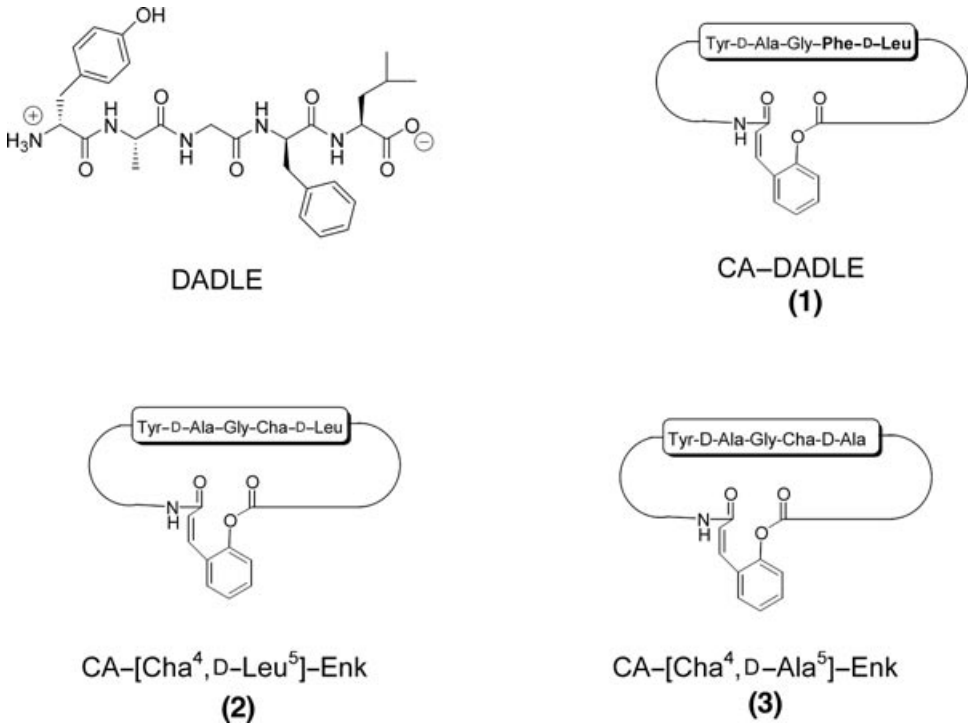

Figure 1. DADLE, CA–DADLE, and modified prodrugs of the cyclic opioid peptide CA–DADLE.

cyclic prodrug [CA–DADLE (**1**)] of the opioid peptide DADLE in which the N- and C-termini of the peptide are joined via chemical linkers, specifically the coumarinic acid linker (CA; Fig. 1).[17] Unlike the zwitterionic DADLE, the resultant cyclic prodrug is uncharged at physiological pH and it is lipophilic rather than hydroplilic.[17–19] However, this cyclic DADLE prodrug did not show the expected increased cell permeation.[13,15,20,21] Using cell culture models, it was shown that the cyclic prodrug is a substrate for apically polarized efflux transporters [e.g., P-glycoprotein (P-gp)] in the intestinal mucosa.[13,17,22–25] Considering the fact that many P-gp substrates are also substrates for cytochrome P450 (CYP450) enzymes,[26–29] it was not unexpected to find that CA–DADLE undergoes rapid oxidative metabolism in the presence of liver microsomes and human recombinant cytochrome P450 3A4 (hCYP3A4).[21]

In this paper, we describe the main sites of oxidative metabolism on CA–DADLE (e.g., Tyr^1 and Phe^4). Using this knowledge and our general understanding of the structure–activity relationship of opioid peptides,[30–35] two new CA–DADLE analogs were designed and synthesized (Fig. 1). Specifically, chemical modifications of the amino acid sequence of DADLE were made creating the new cyclic prodrugs, CA–[Cha^4,D-Leu^5]–Enk (**2**) and CA–[Cha^4,D-Ala^5]–Enk (**3**). Ultimately, synthesis of these new cyclic prodrug analogs will allow us to probe the effect modification of Phe^4 has on oxidative metabolism and cell permeation. In the studies described in this paper, the site of oxidative metabolism on CA–DADLE was elucidated, and the design and synthesis of two new CA–DADLE analogs are reported, as well as their metabolism by animal and human microsomes and a cloned human CYP450.

MATERIALS AND METHODS

The cyclic prodrug CA–DADLE (**1**) was synthesized in our laboratory following described procedures.[8,12] Pooled male Sprague–Dawley rat liver microsomes (RLM); pooled, male Hartley albino guinea pig liver microsomes (GPLM); pooled, mixed-gender human liver microsomes (HLM); and hCYP3A4 expressed in bactosomes with reductase +b5 were purchased from Xenotech, LLC (Lenexa, Kansas). DADLE, diethyl *p*-nitrophenyl phosphate (paraoxon), ketoconazole, β-nicotinamide adenine dinucleotide phosphate (β-NADPH; reduced form), sodium phosphate monobasic (NaH_2PO_4), and sodium phosphate dibasic (Na_2HPO_4) were obtained from Sigma–Aldrich (St. Louis, Missouri). Lindlar's catalysis was purchased from Fluka Chemical Corporation (Milwaukee, Wisconsin). Amino acids were purchased from Novabiochem (La Jolla, California), and the final coupling reagent, *N*-*N*-bis(2-oxo-3-oxozolidinyl)-phosphinic chloride was purchased from TCI-America (Portland, Oregon). Silica gel (Selecto Scientific;

 DOI 10.1002/jps

Suwanee, Georgia)) and solvents [high-performance liquid chromatography (HPLC) grade] were purchased from Fisher Scientific (Pittsburgh, Pennsylvania). All other chemicals were purchased from Sigma–Aldrich. Tetrahydrofuran (THF) was distilled over sodium metal in the presence of benzophenone. Dichloromethane (CH_2Cl_2) was distilled over calcium hydride. All other chemicals and solvents were used as received. During the synthesis process, nuclear magnetic resonance (NMR) spectra were taken on a 400-MHz instrument. The identity of the final cyclic prodrug products were confirmed with a Quattro Micro triple quadrupole mass spectrometer using positive-mode electrospray ionization (ESI+)(Waters; Milford, Massachusetts).

In Vitro Microsomal Stability

The *in vitro* stability studies were preformed as previously described in our laboratory, with only minor modifications.[36] Briefly, the metabolic stability studies of the cyclic prodrugs **1**–**3** were preformed in 500 μL of phosphate buffer solution (100 mM, pH 7.4) containing 2.5 μM of cyclic peptide prodrug, 1 mM NADPH, and 300 nM CYP450 enzyme from RLM, GPLM, or HLM, or 20 nM hCYP3A4. The solution was incubated for 15 min at 37°C with and without inhibitors (100 μM paraoxon and/or 5 μM ketoconazole). The mixture was quenched with a stop solution [100 μL of methanol and 750 μL of acetonitrile (ACN)] and then vortexed to thoroughly mix, followed by centrifugation at 13,000*g* for 15 min. The supernatant (500 μL) was removed and evaporated to dryness (CentriVap concentrator; Labconco, Kansas City, Missouri). The sample was reconstituted in 100 μL of 25% ACN and analyzed using liquid chromatography–tandem mass spectrometry (LC –MS/MS). Side-by-side control experiments were performed to monitor non-enzyme-mediated degradation. For the control experiments, methanol (100 μL) was added to the buffer–NAPDH–prodrug solution before the addition of hCYP3A4 or microsomes. After the addition of hCYP3A4 or microsomes, the reaction was quickly stopped with 750 μL of ACN and processed as stated above. The amount of substrate remaining was calculated by dividing the average substrate peak area by the average substrate peak area in the control sample. Statistics were performed with SigmaStat 3.5 (Systat Software, Inc; Chicago, Illinois) using a one-way ANOVA with a Hohn–Sidik multiple comparison.

Metabolite Identification

Oxidative metabolites of the cyclic prodrugs **1**–**3** were determined in 500 μL of phosphate buffer (100 mM, pH 7.4) containing 50 μM cyclic peptide prodrug, 5 mM NADPH, and 300 nM P450 enzyme from RLM, GPLM, or HLM; or 20 nM hCYP3A4 bactosomes. The solution was incubated for 60 min at 37°C and then quenched with a stop solution (100 μL of methanol and 750 μL of ACN). The mixture was vortexed and then centrifuged at 13,000*g* for 15 min. The supernatant (500 μL) was removed and evaporated to dryness (CentriVap concentrator; Labconco). The sample was reconstituted in 100 μL of 25% ACN for analysis.

Analytical Methods

The metabolic stability and metabolite identification samples were assayed using HPLC in tandem with LC–MS/MS. Separation was preformed on a Waters 2690 HPLC system and a Quattro Micro triple quadrupole mass spectrometer was employed using ESI+ (Waters; Milford, Massachusetts). The compounds were eluted on a Vydac C18 column (50 × 1.0 mm^2 internal diameter, 300 Å) (Alltech; Deefield, Illinois) employing a binary gradient [solvent A, water with 0.1% formic acid (v/v); solvent B, acetronitrile with 0.1% formic acid (v/v)]. The total run time was 20 min, with a flow rate of 0.2 mL/min (3 min gradient from 5% to 40% B; 3 min gradient from 40% to 95% B; 2 min hold at 95%; 2 min return to 5% B; 10 min equilibration at 5% B). For metabolic stability studies, multiple reaction monitoring (MRM) scans were used to determine the presence of the cyclic prodrug parent and the linear peptide using the following *m/z* transitions: parent > 136.1 (Tyr) with parent *m/z* set at 698.4 {CA–DADLE (**1**)}, 704.2 {CA–[Cha^4,D-Leu^5]–Enk (**2**)}, and 662.6 {CA–[Cha^4,D-Ala^5]–Enk (**3**)}. The oxidative metabolites for CA–DADLE were identified using MRM scans with the following *m/z* transitions: parent > 102.6, 136.1, 152.2, and 223.0, with parent *m/z* set at 714.4 (CA–DADLE + OH). The oxidative metabolites of the CA–DADLE analogs were identified with the following *m/z* transitions: parent > 102.6, 142.0, 152.2, and 223.0 with parent *m/z* set at 720.3 (CA–[Cha^4,D-Leu^5]–Enk + OH) and 678.6 (CA–[Cha^4,D-Ala^5]–Enk + OH).

Synthesis

Standard Solution-Phase Peptide Synthesis Using t-Butoxy Carbonyl–Amino Acid Chemistry.

Coupling. The *t*-butoxy carbonyl (Boc)-protected amino acid (26 mmol) was dissolved in dry THF (300 mL) and put on ice. To this solution, 1-(3-dimethylaminopropyl)-3-ethylcarbodiimide hydrochloride (EDC-HCl; 7 g, 37 mmol) and 1-hydroxybenzotriazole (HOBt; 5.7 g, 42 mmol) were added. The solution was stirred for 5 min, and then to this solution, triethyl amine (TEA; 5.6 g, 55 mmol), 4-dimethylamino pyridine (DMAP; 353 mg, 3 mmol), and C-terminal-protected peptide (30 mmol) were added. The reaction was stirred at room temperature for 5 h. The THF was evaporated under vacuum. Purification was preformed via extraction, where 500 mL of ethyl acetate was used to dissolve the residue. The

ethyl acetate solution was extracted with an acid solution [10% citric acid (3 × 200 mL)] followed by a base solution [5% sodium bicarbonate ($NHCO_3$) solution (3 × 200 mL)]. A final wash with saturated brine (1 × 200 mL) was preformed before magnesium sulfate ($MgSO_4$) was used to dry the organic layer. The $MgSO_4$ was filtered off and the collected ethyl acetate was evaporated, resulting in the desired peptide. Further purification (unless noted) was not preformed until final protected peptide chain had been synthesized.

Boc Deprotection. The Boc-protected peptide (34.3 mmol) was dissolved in ethyl acetate (50 mL) and cooled to 0°C. HCl gas was bubbled through the solution for 15 min. The gas was removed, and the reaction was stirred for an additional 15 min at 0°C. The solvent was evaporated under vacuum. Further purification (unless noted) was not preformed until final protected peptide chain had been synthesized

Peptide Arm

Boc–D-Ala–Gly–OAll (**4**). Yield: 100%. $R_f = 0.51$ (chloroform/methanol, 3:1). ^{1}H NMR (400 MHz, $CDCl_3$) δ 1.28 (d, 3H, $J = 7.0$), 1.34 (s, 9H), 3.96 (m, 2H), 4.21 (s, 1H), 4.53 (d, 2H, $J = 5.6$), 5.13 (d, 1H, $J = 10.4$), 5.21 (d, 1H, $J = 17.2$), 5.54 (s, 1H), 5.79 (m, 1H). ^{13}C NMR (400 MHz, $CDCl_3$) δ 28.22, 41.08, 49.85, 79.67, 118.63, 124.85, 128.73, 131.48, 143.25, 155.49, 169.4, 173.6.

H–D-Ala–Gly–OAll (**5**). Yield: 100%. $R_f = 0.12$ (CH_2Cl_2/methanol/acetic acid, 20:3:0.1). ^{1}H NMR (400 MHz, MeOD) δ 1.56 (d, 3H, $J = 5.8$), 3.99 (m, 2H), 4.59 (d, 2H, $J = 4.8$), 5.18 (d, 1H, $J = 10.3$), 5.27 (d, 1H, $J = 17.1$), 5.89 (m, 1H). ^{13}C NMR (400 MHz, $CDCl_3$) δ 40.74, 49.03, 65.55, 117.58, 131.9, 169.29, 170.39.

Boc–Tyr–D-Ala–Gly–OAll (**6**). Yield: 100%. $R_f = 0.23$ (chloroform/ACN, 3:1). ^{1}H NMR (400 MHz, $CDCl_3$) δ 1.20 (d, 3H, $J = 6.5$), 1.37 (s, 9H), 2.91 (m, 2H), 4.05 (dd, 2H, $J_1 = 17.4$, $J_2 = 52.3$), 4.16 (m, 1H), 4.33 (d, 1H, $J = 7.2$), 4.61 (d, 2H, $J = 5.6$), 5.21 (dd, 1H, $J_1 = 1.2$, $J_2 = 10.5$), 5.31 (dd, 1H, $J_1 = 1.5$, $J_2 = 17.2$), 5.93 (m, 1H), 6.72 (d, 2H, $J = 8.5$), 7.04 (d, 2H, $J = 8.3$). ^{13}C NMR (400 MHz, MeOD) δ 17.58, 28.28, 41.27, 48.62, 56.64, 66.05, 80.32, 115.63, 118.94, 127.39, 130.32, 131.43, 155.55, 155.85, 169.67, 172.06, 172.87.

Boc–Tyr–D-Ala–Gly–OH (**7**). To remove the C-terminal Allyl group, peptide **6** (8.7 g, 20 mmol) was dissolved in 50 mL dry THF. To this solution, tetrakis (triphenylphosphine) Palladium [$Pd(PPh_3)_4$] (2.3 g, 2 mmol) and morpholine (17 mL, 200 mmol) were added. The reaction was then stirred at room temperature for 90 min. The THF was evaporated under vacuum, and the residual oil was purified by silica gel column chromatography with chloroform/methanol (3:1). $R_f = 0.11$ (chloroform/methanol, 3:1). Yield: 46%. ^{1}H NMR (400 MHz, MeOD) δ 1.21 (t, 3H $J_1 = 7.0$, $J_2 = 14.1$) 1.10 (s, 9H), 2.92 (m, 2H), 3.69 (dd, 2H, $J_1 = 17.1$, $J_2 = 76.0$), 4.21 (s, 1H), 4.31 (m, 1H), 6.72 (d, 2H, $J = 7.7$), 7.05 (d, 2H, $J = 7.7$). ^{13}C NMR (400 MHz, MeOD) δ17.01, 27.37, 36.88, 42.55, 56.95, 79.46, 114.86, 127.44, 130.02, 155.99, 156.42, 173.21, 173.45.

Boc–Tyr–D-Ala–Gly–Cha–OAll (**8**). Yield: 100%. $R_f = 0.78$ (chloroform/methanol, 3:1). ^{1}H NMR (400 MHz, MeOD) 0.91 (m, 2H), 1.25 (m, 6H), 1.41 (s, 9H), 1.71 (m, 7H), 2.90 (m, 2H). 3.90 (m 2H), 4.14 (m, 1H), 4.52 (m, 1H0, 4.61(m, 2H), 5.31 (dd, 2H, $J_1 = 1.4$, $J_2 = 17.2$), 5.91 (m, 1H), 6.72 (d, 2H $J = 8.3$), 7.03 (d, 2H, $J = 8.2$). ^{13}C NMR (400 MHz, MeOD) δ15.72, 25.72, 25.97, 26.17, 27.42, 31.86, 33.35, 33.79, 38.62, 42.02, 49.48, 50.20, 56.91, 65.28, 79.45, 114.83, 117.29, 127.37, 130.02, 131.96, 156.01, 156.54, 170.22, 172.27, 173.27, 173.94.

H-Tyr–D-Ala–Gly–Cha–OAll (**9**). Yield: 100%. $R_f = 0.68$ (chloroform/methanol, 3:1). ^{1}H NMR (400 MHz, MeOD) δ 0.95 (m, 2H), 1.25 (d, 3H, $J = 7.2$), 1.40 (m, 1H), 1.70 (m, 7H), 3.07 (m, 2H), 3.91 (s, 2H), 4.10 (t, 1H, $J_1 = 7.5$, $J_2 = 15.0$), 4.25 (d, 1H, $J = 7.2$), 4.55 (dd, 1H, $J_1 = 6.5$, $J_2 = 8.4$), 4.62 (s, 2H), 5.23 (d, 1H $J = 10.5$), 5.31 (d, 1H, $J = 17.2$), 5.92 (m, 1H), 6.80 (d, 2H $J = 8.3$), 7.11 (d, 2H $J = 8.3$). ^{13}C NMR (400 MHz, MeOD) δ16.04, 25.72, 25.93, 26.13, 31.89, 33.29, 33.88, 36.28, 38.74, 41.81, 49.58, 50.10, 54.80, 65.47, 115.38, 117.43, 124.69, 130.22, 131.86, 156.88, 168.73, 170.07, 170.15, 172.67, 173.56.

CA Linker. Phenacyl 3-(2-hydroxyphenyl)-propynoate (**10**): Compound **10** was synthesized using a method previously described.[17] ^{1}H NMR (400 MHz, $CDCl_3$) δ 5.52 (s,2H), 6.93 (t, 1H, $J_1 = 7.5$, $J_2 = 16.1$), 7.00 (d, 1H, $J = 8.4$), 7.39 (t, 1H, $J_1 = 8.3$, $J_2 = 17.4$), 7.49 (m, 3H), 7.64 (t, 1H, $J_1 = 7.4$, $J_2 = 13.7$), 7.94 (d, 2H, $J = 9.5$). ^{13}C NMR (400 MHz, $CDCl_3$) δ 67.18, 83.69, 83.33, 105.84, 115.96, 120.69, 127.87, 128.99, 133.38, 133.75, 133.83, 134.22, 153.14, 159.07, 191.02.

Phenacyl 3-(2′-Boc-alacylocyl hydroxyphenyl)-propynoate (**11**): Phenacyl 3-(2-hydroxylphenyl)-propynoate (**10**; 1 g, 3.7 mmol) was dissolved in 40 mL of dry CH_2Cl_2. In another flask containing 10 mL of dry CH_2Cl_2, Boc–D-Ala–OH (840 mg, 4.4 mmol), EDC-HCl (707 mg, 3.7 mmol), and DMAP (452 mg, 3.7 mmol) were dissolved. The mixture was stirred at 0°C for 5 min. The solution with compound **10** was transferred to the flask containing the activated amino acid via cannula and stirred at 0°C for 5 h. CH_2Cl_2 was removed under vacuum. Initial purification was preformed via extraction, where 200 mL of ethyl acetate was used to dissolve the residue. The ethyl acetate solution was extracted with an acid solution [10% citric acid (3 × 100 mL)] followed by a base solution [5% $NHCO_3$ solution (3 × 100 mL)]. A final wash with saturated brine

 DOI 10.1002/jps

(1 × 100 mL) was preformed before $MgSO_4$ was used to dry the organic layer. The $MgSO_4$ was filtered off and the organic layer was evaporated to foam (1.05 g, 66%). The foam was further purified by silica gel column chromatography with chloroform/ethyl acetate (20:1) to give a yellowish oil (750 mg, 47%). $R_f = 0.37$ (chloroform/ ethyl acetate, 20:1). ^{1}H NMR (400 MHz, $CDCl_3$) δ 1.46 (s, 9H), 1.68 (d, 3H, J = 7.28), 4.64 (m, 1H), 5.31 (m, 1H), 5.48 (s, 2H), ^{13}C NMR (400 MHz, $CDCl_3$) δ 17.99, 28.29, 49.56, 67.15, 79.82, 82.52, 84.48, 85.20, 113.51, 122.75, 126.32, 127.77, 128.92, 132.41, 133.77, 134.26, 152.78, 155.36, 171.29, 190.76.

Phenacyl 3-(2′-Boc-alacylocyl hydroxyphenyl)-propenoate (**12**): Phenacyl 3-(2′-Boc-alacylocyl hydroxyphenyl)-propynoate (**11**; 750 mg, 1.72 mmol) was dissolved in absolute ethanol (60 mL). To this, Lindlar catalyst [5 wt% of palladium on calcium carbonate, poisoned with lead; 10% (w/w), 75 mg] and quinoline [2% (w/w), 15 mg] were added. The reaction was stirred at 0°C. Hydrogen gas was bubbled through the solution for 30 min. The HCl gas was removed, and the reaction, which was monitored by ^{1}H NMR, was stirred under a hydrogen atmosphere until complete. Upon completion, the catalyst was removed and the solvent was evaporated under vacuum to give a yellowish foam (680 mg, 82%). The foam was purified by silica gel column chromatography with hexanes/ethyl acetate (4:1) to give a light yellow solid (670 mg, 80%). $R_f = 0.65$ (ethyl acetate/hexanes/methanol, 2:4:1). ^{1}H NMR (400 MHz, $CDCl_3$) δ 1.46 (s, 9H), 1.56 (d, 3H, J = 7.3), 4.53 (t, 1H, $J_1 = 7.2$, $J_2 = 14.5$), 5.37 (d, 2H, $J = 16.4$), 6.22 (d, 1H, $J = 12.2$), 7.08 (m, 2H), 7.21 (t, 1H, $J_1 = 7.6$, $J_2 = 15.2$), 7.32 (m, 1H), 7.46 (m, 2H), 7.59 (m, 2H), 7.87 (d, 2H, $J = 7.2$). ^{13}C NMR (400 MHz, $CDCl_3$) δ 18.35, 28.34, 49.56, 66.09, 79.96, 121.21, 121.74, 125.73, 127.80, 128.83, 129.93, 130.30, 133.92, 134.09, 139.60, 147.86, 155.38, 164.52, 171.62, 192.09.

3-(2′-Boc-alacylocyl hydroxyphenyl)-propenoic (**13**): A mixture of phenacyl 3-(2′-Boc-alacylocyl hydroxyphenyl)-propenoate (**12**; 100 mg, 0.21 mmol) and zinc powder (271 mg, 4.14 mmol) was cooled to 10°C. Acetic acid (22 mL) was slowly added to the reaction. The mixture was stirred at 10°C for 30 min. The supernant was filtered and concentrated under vacuum. The residual oil was purified by silica gel column chromatography with ethyl acetate/hexanes/methanol (2:4:1) to give a colorless oil (90 mg, 75%). $R_f = 0.43$ (ethyl acetate/hexanes/methanol (2:4:1). ^{1}H NMR (400 MHz, MeOD) δ 1.48 (s, 9H), 1.52 (d, 3H, J = 7.3), 4.38 (m, 1H), 6.10 (d, 1H, $J = 12.4$), 6.87 (d, 1H, $J = 12.4$), 7.11 (d, 1H, $J = 8.0$), 7.22 (t, 1H, J_1 = 7.4, $J_2 = 14.6$), 7.35 (t, 1H, $J_1 = 7.6$, $J_2 = 15.2$), 7.64 (d, 1H, $J = 7.3$). ^{13}C NMR (400 MHz, $CDCl_3$) δ 18.07, 28.30, 49.43, 80.25, 121.72, 122.81, 125.78, 128.16, 129.80, 130.47, 137.88.

Compound **14**: A mixture of compound **13** (112 mg, 0.31 mmol), EDC-HCl (82 mg, 0.43 mmol), and HOBt (66 mg, 0.49 mmol) was dissolved in dry THF (6 mL) and stirred at 0°C for 5 min. To this solution, DMAP (4 mg, 0.03 mmol) and TEA (66 mg, 0.64 mmol) were added. In another flask, H-Tyr–D-Ala–Gly–Cha–OAll (**9**; 170 mg, 0.33 mmol) was dissolved in 4 mL dry THF and transferred via cannula to the reaction flask containing compound **13**. The mixture was stirred at room temperature for 6 h. THF was removed under vacuum. Initial purification was preformed via extraction, where 100 mL of ethyl acetate was used to dissolve the residue. The ethyl acetate solution was extracted with an acid solution [10% citric acid (2 × 50 mL)] followed by a base solution [5% $NHCO_3$ solution (2 × 50 mL)]. A final wash with saturated brine (1 × 200 mL) was preformed before $MgSO_4$ was used to dry the organic layer. The $MgSO_4$ was filtered off and the organic layer was evaporated to a yellowish white solid (200 mg, 80%). The solid was further purified by silica gel column chromatography with chloroform/methanol (20:1) to give a white solid (110 mg, 44%). $R_f = 0.26$ (chloroform/methanol, 20:1). ^{1}H NMR (400 MHz, $CDCl_3$) δ 0.87 (m, 2H), 1.16 (m, 6H), 1.40 (s, 9H), 1.53 (d, 3H, $J = 7.2$), 1.63 (m, 7H), 2.55 (m, 1H), 2.74 (m, 1H), 3.90 (m, 2H), 4.35 (m, 2H), 4.59 (m, 3H), 5.24 (d, 2H, $J = 10.4$), 5.33 (d, 2H, $J = 17.3$), 5.85 (m, 1H), 6.10 (d, 1H $J = 12.1$), 6.67 (m, 3H), 6.84 (d, 2H, $J = 7.3$), 7.00 (m, 2H), 7.20 (m, 1H), 7.32 (m, 1H). ^{13}C NMR (400 MHz, $CDCl_3$) δ 18.11, 25.91, 26.10, 26.36, 28.37, 32.32, 33.40,33.92, 39.40,49.33, 50.35, 65.85, 80.33, 115.65, 118.70, 121.88, 126.52, 127.15, 129.01, 130.28, 131.61, 147.80, 155.51, 166.84, 169.65, 172.59, 173.01.

Compound 15. Removal of Allyl group: Compound **14** (110 mg, 0.13 mmol) was dissolved in 10 mL dry THF. To this solution, $Pd(PPh_3)_4$ (15.5 mg, 1.0 mmol) and morpholine (117 mg, 1.34 mmol) were added. The reaction was then stirred at room temperature for 90 min. The THF was evaporated under vacuum and the residual oil was purified by silica gel column chromatography with chloroform/methanol (3:1). $R_f = 0.43$ (chloroform/methanol, 3:1).

Removal of Boc-group: The —OAll deprotected product from above was dissolved in ethyl acetate (60 mL) and cooled to 0°C. HCl (gas) was bubbled through the solution for 10 min. The HCl gas was removed, and the solution was stirred for another 10 min at 0°C. Vacuum was used to evaporate the solvent, yielding a white solid (**15**) to which no further purification was preformed. Total yield for these two deprotection steps was 49%. $R_f = 0.47$ (chloroform/methanol, 20:1). ^{1}H NMR (400 MHz, MeOD) δ 0.94 (m, 2H), 1.17 (d, 3H,

$J = 7.3$), 1.43 (m, 1H), 1.57 (m, 1H), 1.72 (d, 3H, $J = 7.1$), 1.76 (m, 7H), 2.87 (d, 2H, $J = 7.5$), 3.66 (dd, 2H, $J_1 = 16.8$, $J_2 = 50.6$), 3.86 (m, 1H), 4.30 (m, 1H), 4.40 (m, 2H), 6.25 (d, 1H, $J = 12.1$), 6.72 (d, 2H, $J = 8.3$), 6.83 (d, 1H, $J = 12.2$), 7.01 (d, 2H, $J = 8.1$), 7.17 (d, 1H, $J = 8.5$), 7.23 (t, 1H, $J_1 = 7.3$, $J_2 = 14.7$), 7.38 (d, 2H, $J = 7.4$). ^{13}C NMR (400 MHz, MeOD) δ 19.38, 25.70, 25.97, 26.18, 31.83, 33.43, 33.81, 36.17, 38.92, 42.06, 48.66, 56.10, 60.15, 114.87, 121.33, 125.53, 126.13, 126.85, 129.05, 129.15, 129.91, 130.13, 133.25, 147.13, 156.12, 166.79, 168.31, 170.40, 172.70.

CA–[Cha^4,D-Ala^5]–Enk (**2**). Compound **15** was initially dissolved in 1 mL anhydrous *N*,*N*-dimethylformamide, and then 50 mL of CH_2Cl_2 was slowly added. To this solution, TEA (30 mg, 0.3 mmol) and bis(2-oxo-3-oxazolidinyl) phosphinic chloride (53 mg, 0.21 mmol) were added. A cloudy mixture resulted, and the reaction was stirred at room temperature for 18 h. The resultant clear yellow solution was evaporated under vacuum to give a yellow solid. The solid was dissolved in ethyl acetate (10 mL) and washed with another 10 mL of water. The ethyl acetate layer was collected and washed with 10% citric acid (1 × 10 mL) and 5% $NaHCO_3$ solution (1 × 10 mL). The organic layer was collected, dried with $MgSO_4$, filtered, and evaporated to a clear oil. The oil was purified by semi-preparative HPLC with ultraviolet detection. The eluate was analyzed by ESI–MS, and fractions containing peptide prodrug were pooled. The pooled fractions were lyophilized, resulting in a white solid (6.7 mg, 34%). Semi-preparative HPLC was carried out using a C18 Dynamax column (300 Å)(Agilent; Santa Clara, California). The cyclic peptide prodrug was isolated using a gradient from 10% to 100% B (solvent A, 90% water with 0.01% formic acid; solvent B, 90% ACN with 0.01% formic acid). The gradient was applied stepwise for a total run time of 121 min, with a flow rate of 5 mL/min (16 min gradient from 10% to 30% B; 10 min gradient from 30% to 40% B; 40% B for 10 min; 15 min gradient from 40% to 45% B; 10 min gradient from 45% to 100% B; 15 min at 100% B; 15 min return to 10% B; 30 min equilibration at 10% B). The peptide prodrug had a retention time of about 45 min. $R_f = 0.22$ (chloroform/methanol, 20:1) ^{1}H NMR (400 MHz, MeOD) δ 0.99 (m, 4H), 1.20 (d, 3H, $J = 7.3$), 1.25 (m, 9H), 1.56 (d, 3H, $J = 7.4$), 1.74 (m, 7H), 2.85 (m, 2H), 3.88 (m, 2H), 4.03 (m, 1H), 4.28 (m, 1H), 4.46 (m, 1H), 4.65 (m, 1H), 6.20 (d, 1H, $J = 12.1$), 6.70 (d, 2H, $J = 8.5$), 6.78 (d, 1H, $J = 12.0$), 6.97 (d, 2H, $J = 8.3$), 7.07 (m, 1H), 7.23 (m, 1H), 7.36 (m, 2H). ESI–MS *m/z* 662.6 (M + 1).

CA–[Cha^4,D-Leu^5]–Enk (**1**). ^{1}H NMR (500 MHz, MeOD-d_4) δ 1.37 (dd, 6H, $J_1 = 6.0$, $J_2 = 17.3$), 1.57 (d, 3H, $J = 7.3$), 1.65 (m, 3H), 1.82 (m, 2H), 2.11 (m, 9H), 3.10 (dd, 1H, $J_1 = 7.3$, $J_2 = 13.7$), 3.21 (m, 1H), 4.18 (d, 1H, $J = 17.1$), 4.31 (dd, 1H, $J_1 = 7.3$, $J_2 = 14.6$) 4.68 (t, 1H, $J_1 = 7.7$, $J_2 = 15.1$), 4.86 (dd, 1H, $J_1 = 5.5$, $J_2 = 10.0$), 5.05 (m, 1H), 6.55 (d, 1H, $J = 12.1$), 7.06 (d, 2H, 8.5), 7.14 (d, 1H, $J = 12.1$), 7.28 (d, 2H, $J = 8.4$), 7.42 (d, 1H, $J = 8.0$), 7.60 (m, 2H), 7.73 (m, 1H). ESI–MS *m/z* 704.5 (M + 1).

RESULTS

Synthesis

The synthesis and characterization of the new CA–DADLE analogs (Fig. 1) was undertaken using the methodology developed previously in our laboratory.[17] The synthetic design for the new cyclic prodrugs was based on retrosynthetic analysis leading back to two fundamental pieces, the peptide arm and a CA moiety (Fig. 2). The peptide arm was synthesized utilizing standard solution-phase Boc–amino acid chemistry, an example of which is described in Figure 3. L-amino acids were used unless otherwise designated. The general synthesis of the CA base (**10**) is reported elsewhere.[17] Using standard peptide-coupling chemistry, the CA base was further modified to incorporate the fifth amino acid of the peptide sequence forming the linker moiety (Fig. 4). After protection and deprotection steps, the linker moiety was coupled with the peptide arm to form the linear precursor (Fig. 4). The final step in the synthesis of the cyclic prodrugs was cyclization of the linear precursor. This step forms the final peptide bond between the fourth

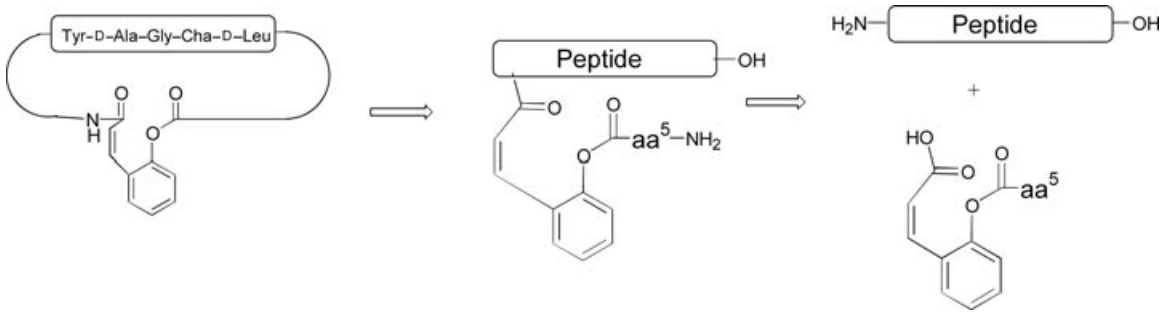

Figure 2. Retrosynthetic analysis leading to the peptide arm and coumarinic acid linker fragments. aa, amino acid.

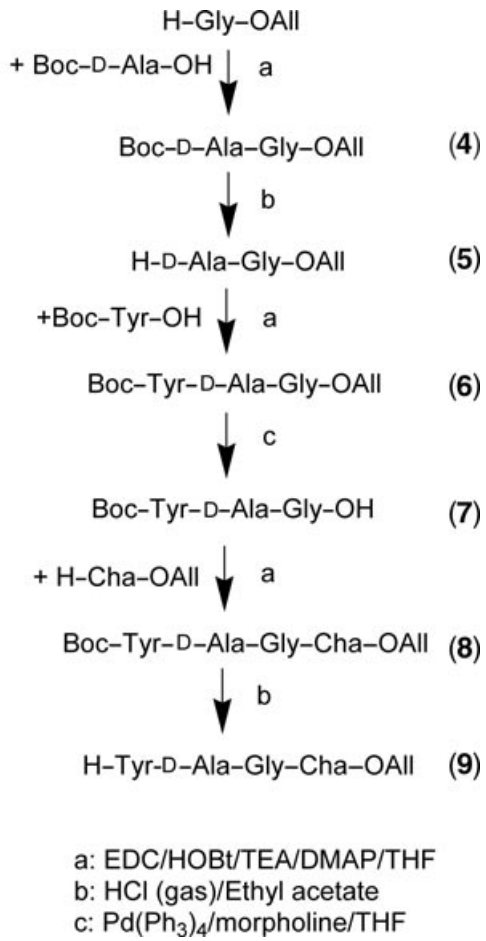

Figure 3. Synthesis of one of the peptide arms, a fundamental building block for the synthesis of cyclic prodrugs.

and fifth amino acids in the peptide sequence and yields a cyclic final product (Fig. 4). The synthetic intermediates were confirmed by ^{1}H and ^{13}C NMR. The structural identities of the cyclic prodrugs were verified by ^{1}H NMR and ESI–MS.

In Vitro Microsomal Stability

The metabolic characteristics of DADLE and cyclic prodrugs of DADLE were investigated using RLM, GPLM, HLM, or hCYP3A4 in the presence or absence of specific enzyme inhibitors (e.g., paraoxon, an esterase B inhibitor; or ketoconazole, a CYP450 inhibitor). As shown in Figure 5, DADLE is metabolically stable when incubated with RLM in the absence or presence of paraoxon and/or ketoconazole. In contrast, the DADLE cyclic prodrugs **1**–**3** show significant metabolic instability when incubated with RLM (i.e., CA–DADLE, CA–[Cha^4,D-Leu^5]–Enk, and CA–[Cha^4,D- Ala^5]–Enk show only 20%, 48%, and 17% of cyclic prodrug remaining, respectively, after a 15 min incubation). Inclusion of paraoxon in the incubation mixture did little to improve the metabolic stability of the cyclic prodrugs (i.e., CA–DADLE, CA–[Cha^4,D-Leu^5]–Enk, and CA–[Cha^4,D- Ala^5]–Enk show only 27%, 60%, and 27% of cyclic prodrug remaining, respectively, after a 15 min incubation). The addition of ketoconazole alone or ketoconazole and paraoxon to the incubation mixture significantly decreased the metabolism of the three cyclic prodrugs. As shown in Figure 5, more than 90% of the cyclic prodrugs **1**–**3** were detected after a 15 min incubation.

When incubated in the presence of GPLM, more than 90% of the DADLE was detected after a 15 min incubation with or without paraoxon and/or ketoconazole (Fig. 6). However, the cyclic prodrugs **1**–**3** were very unstable when incubated with GPLM (i.e., 6% of CA–DADLE, 34% of CA–[Cha^4,D-Leu^5]–Enk, and 8% CA–[Cha^4,D-Ala^5]–Enk were detected after a 15 min incubation). Inclusion of paraoxon did little to enhance the metabolic stability of CA–DADLE, CA–[Cha^4,D-Leu^5]–Enk, and CA–[Cha^4,D-Ala^5]–Enk, with only 11%, 42%, and 11%, respectively, of cyclic prodrug remaining after a 15 min incubation. However, inclusion of ketoconazole in the incubation mixture dramatically increased the stability of the cyclic prodrugs (i.e., >70% of prodrugs **2** and **3**, and 44% of prodrug **1** were present after incubation with GPLM). The results from inclusion of ketoconazole and paraoxon to the incubation mixture were similar to the results observed with ketoconazole alone (i.e., >65% of the cyclic prodrugs **1**–**3** remained after the 15 min incubation with GPLM).

The metabolic stability of cyclic prodrugs **1** and **2** when incubated with HLM were similar to the results observed with RLM and GPLM. DADLE is stable under all conditions, showing a significant amount of the opioid peptide remaining after a 15 min incubation with HLM (Fig. 7). Contrary to DADLE, the cyclic prodrugs **1**–**3** were unstable in the presence of HLM, with only 15%, 50%, and 20% remaining of CA–DADLE, CA–[Cha^4,D-Leu^5]–Enk, and CA–[Cha^4,D-Ala^5]–Enk, respectively (Fig. 7). The metabolic stability of the cyclic prodrugs **1**–**3** is increased significantly with the addition of ketoconazole (>80% remaining after a 15 min incubation), but remains low with the addition of paraoxon (<20% remaining after a 15 min incubation; Fig. 7). Inclusion of ketoconazole and paraoxon to the HLM incubation mixture resulted in more than 90% recovery of the cyclic prodrugs **1**–**3**.

The cyclic prodrugs showed significantly different metabolic stability profiles when incubated with hCYP3A4 (Fig. 8). CA–DADLE did not exhibit high stability in the presence of hCYP3A4 in the absence of inhibitors, with only 9% of the parent drug remaining under this condition. The CA–DADLE analogs **2** and **3**, however, displayed relatively high metabolic stability in the presence of hCYP3A4.

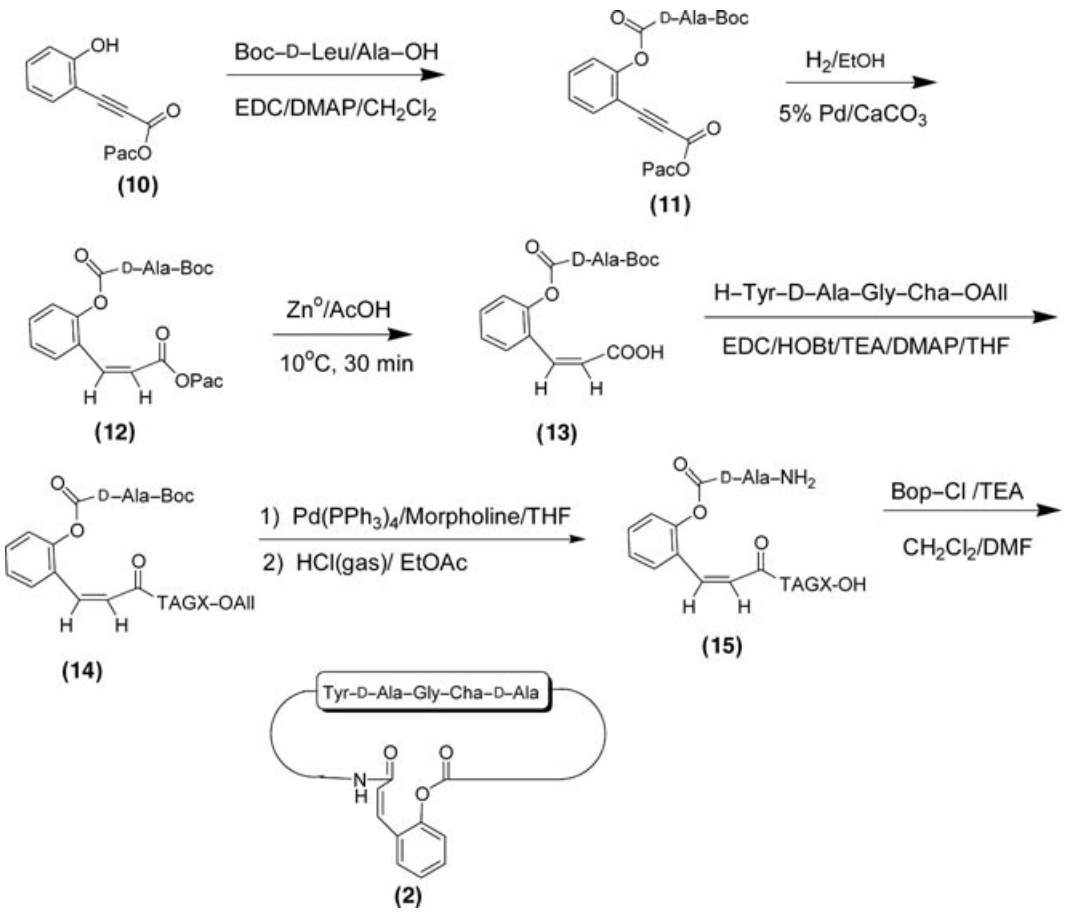

Figure 4. Final synthetic route to CA–[Cha[4],D-Ala[5]]–Enk (**2**), including the addition of the fifth amino acid to the basic linker moiety and formation of the linear precursor Tyr-D-Ala-Gly-Cha.

The data show 78% of the cyclic parent remaining for CA–[Cha[4],D-Leu[5]]–Enk and 87% remaining for CA–[Cha[4],D-Ala[5]]–Enk. The addition of ketoconazole did improve the metabolic stability of CA–DADLE fivefold, but had relatively little effect on the metabolic stability of the CA–DADLE analogs **2** and **3**. DADLE shows high stability in the presence of hCYP3A4, with more than 98% of the parent remaining with and without inhibitors.

Metabolite Identification

DADLE, the cyclic prodrugs **1**–**3**, and their metabolites have been analyzed by LC–MS/MS. For all compounds, similar common immonium product ions resulted (Fig. 9). The *m/z* ratio of these common product ions correlate with portions of the peptide that contain various amino acid fragments. The fragmentation shows peaks at *m/z* of 86.6, 120.1 (or 126.0),

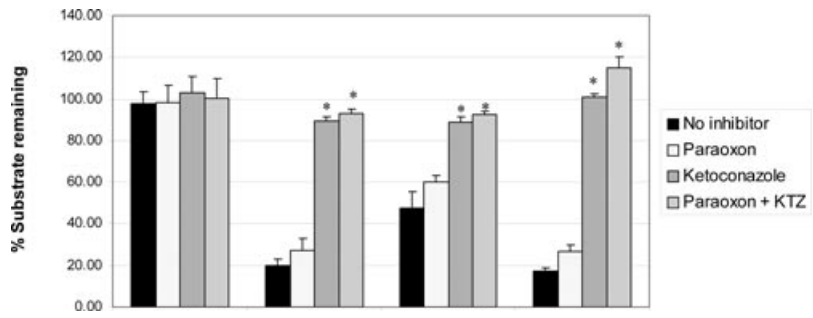

Figure 5. Stability of DADLE and the cyclic prodrugs CA–DADLE (**1**), CA–[Cha[4],D-Leu[5]]–Enk (**2**), and CA–[Cha[4],D-Ala[5]]–Enk (**3**) in the presence of rat liver microsomes with and without inhibitors after 15 min incubation ($*p < 0.001$). KTZ, ketoconazole.

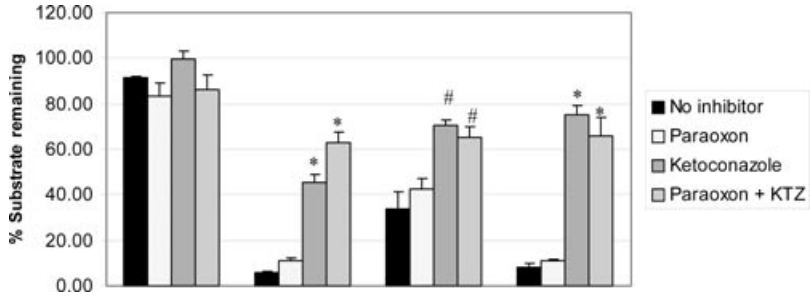

Figure 6. Stability of DADLE and the cyclic prodrugs CA–DADLE (**1**), CA–[Cha^4,D-Leu^5]–Enk (**2**), and CA–[Cha^4,D-Ala^5]–Enk (**3**) in the presence of guinea pig liver microsomes with and without inhibitors after 15 min incubation ($^*p < 0.001$ and $\#p < 0.003$). KTZ, ketoconazole.

136.2, and 207.0 (Fig. 9). These fragments are related to the peptide portion of these prodrugs and have been identified as Leu, Phe (or Cha), Tyr, and a dipeptide fragment, Tyr–Ala, respectively. In the cyclic prodrug spectra, there was an additional product ion peak identified at *m/z* 147.0, which corresponds to the coumarin linker of the cyclic prodrugs. The metabolic stability of the CA in the presence of animal and human microsomes or hCYP3A4 has been confirmed [i.e., hydroxylated coumarins have not been observed, and only *m/z* 147 has been detected (data not shown)]. With the common product ions identified for both the linear and cyclic prodrugs, the MRM transitions of oxidative metabolites of the cyclic prodrugs could be predicted.

After incubation of the cyclic prodrugs with RLM, GPLM, HLM, or hCYP3A4, the oxidative product ions were identified using MRM. The oxidized product ions being investigated had *m/z* ratios of 102.6, 136.1 (or 142.0), 152.2, and 223.0 corresponding to the previously determined product ions with the addition of a hydroxyl group. It should be noted that with this method, only the amino acid undergoing oxidation can be identified. The exact location of the hydroxyl group on the amino acid was not determined. Oxidation leading to the addition of two or three hydroxyl groups was not seen under any of the experimental conditions studied. Also, when no oxidative metabolites were detected, the original unoxidized molecule was observed, confirming the metabolic stability of either DADLE or the cyclic prodrugs.

The metabolite identification studies correlate well with the metabolic stability studies. DADLE was shown to be metabolically stable under the four

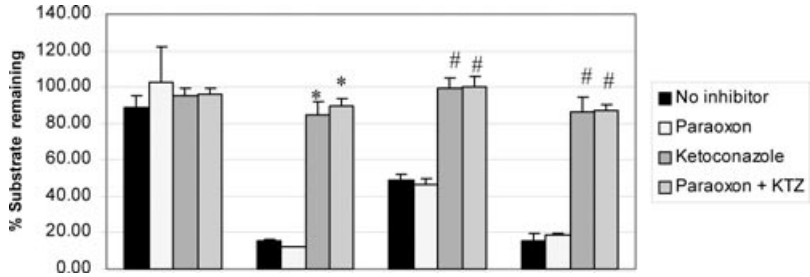

Figure 7. Stability of DADLE and the cyclic prodrugs CA–DADLE (**1**), CA–[Cha^4,D-Leu^5]–Enk (**2**), and CA–[Cha^4,D-Ala^5]–Enk (**3**) in the presence of human liver microsomes (HLM) with and without inhibitors after 15 min incubation ($^*p = 0.022$ and $\#p < 0.001$). KTZ, ketoconazole.

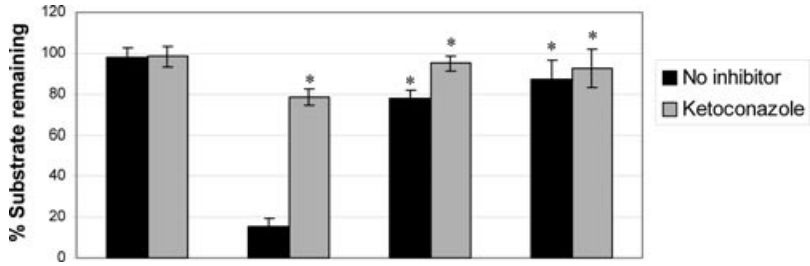

Figure 8. Stability of DADLE and the cyclic prodrugs CA–DADLE (**1**), CA–[Cha^4,D-Leu^5]–Enk (**2**), and CA–[Cha^4,D-Ala^5]–Enk (**3**) in the presence of hCYP3A4 with and without ketoconazole after 15 min incubation ($^*p < 0.001$).

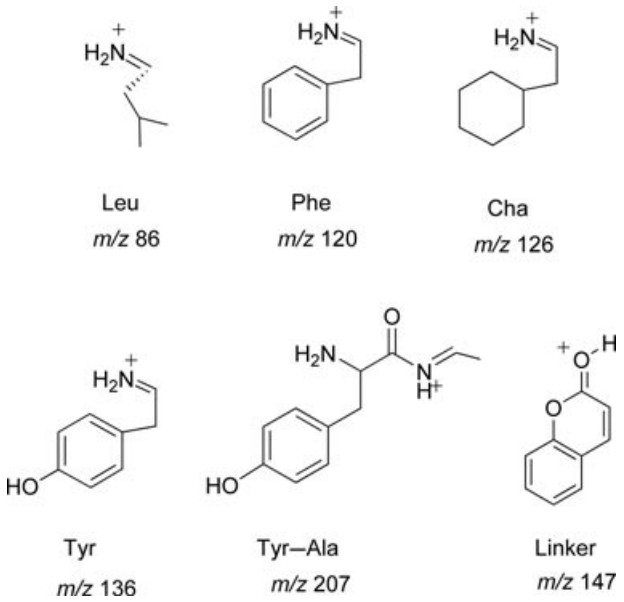

Figure 9. Structures of the common ion products of DADLE and CA–DADLE.

oxidative conditions studied (e.g., incubation with RLM, GPLM, HLM, or hCYP3A4). The metabolism of the cyclic prodrugs **1**–**3** was studied under the same experimental conditions, but yielded very different results. The metabolites arising from the oxidation of CA–DADLE, CA–[Cha^4,D-Leu^5]–Enk, and CA–[Cha^4,D-Ala^5]–Enk are shown in Table 1. These data showed that CA–DADLE is hydroxylated on Tyr^1 or Phe^4 in the presence RLM, but CA–DADLE analogs **2** and **3** showed oxidation on only Tyr^1. Incubations with GPLM yielded similar results for CA–DADLE (e.g., hydroxylation at Tyr^1 or Phe^4). CA–[Cha^4,D-Leu^5]–Enk when incubated with GPLM showed an identical metabolic profile (e.g., hydroxylation at Tyr^1 or Cha^4). However, when CA–[Cha^4,D-Ala^5]–Enk was incubated with GPLM, only the Tyr^1 metabolite was formed. Incubation with HLM yielded the same metabolites as incubation with GPLM for the cyclic prodrug analogs **2** and **3** (e.g., hydroxylation at Tyr^1 or Cha^4 for CA–[Cha^4,D-Leu^5]–Enk (**2**), and Tyr^1 for CA–[Cha^4,D-Ala^5]–Enk). In contrast, CA—DADLE when incubated with HLM generated only one metabolite (e.g., hydroxylation at Tyr^1), not the metabolite arising from hydroxylation of Phe^4. Interestingly, in the presence of hCYP3A4, CA–DADLE yields the metabolite arising from the oxidation at Phe^4 position, whereas cyclic prodrug analogs **2** and **3** showed no significant metabolite formation under the same experimental conditions.

DISCUSSION

Synthetic Strategy

Previously, our laboratory has reported that in spite of optimal physicochemical properties, cyclic prodrugs of DADLE, formed using different chemical linkers, do not exhibit increased cell membrane permeation when compared with the linear opioid peptide permeation.[12,13,20–22,25] The poor cell permeation characteristics of these cyclic prodrugs appear to arise from their substrate activity for efflux transporters and/or their potential to be metabolized by CYP450 enzymes.

In an attempt to improve the permeation properties of one of these cyclic DADLE prodrugs, two structural analogs of CA–DADLE were designed and synthesized. The main goal in designing and synthesizing these CA–DADLE analogs was to stabilize the cyclic prodrug toward oxidative metabolism while still maintaining high affinity for the opioid receptor. Metabolite identification studies described in this paper showed that CA–DADLE was oxidized at the Tyr^1 and/or Phe^4 residues when incubated with animal or human microsomes or a recombinant CYP450 (e.g., hCYP3A4). Because it has been well established that modification of the Tyr^1 residue on opioid peptides dramatically decreases their affinities for the opioid receptor,[31,37,34,35] structural changes to this critical amino acid residue were not attempted in our studies. Instead, a modification at the Phe^4 residue of CA–DADLE was made, which should have had minimal effect on the peptides' affinity for the opioid receptors.[30,33]

One prodrug analog was designed to differ from CA–DADLE by modification of the fourth amino acid residue from Phe^4 to Cha^4, creating CA–[Cha^4,D-Leu^5]–Enk (**2**; Fig. 1). Enkephalin analogs having this type of structural change (e.g., Phe^4 to Cha^4) have been shown to retain opioid-like activity *in vivo*,[30] with only slight modification of the potency and binding affinity for the opioid receptor.[33] Small opioid peptides have also been shown to maintain modest binding affinity to the opioid receptors when Phe^4 to Cha^4 modifications are made in the amino acid sequence.[38–40]

The design of the second analog of CA–DADLE includes the aforementioned Phe^4-to-Cha^4 structural

Table 1. Metabolites Arising from Phase I Oxidation of CA–DADLE, CA–[Cha^4,D-Leu^5]–Enk, and CA–[Cha^4,D-Ala^5]–Enk

Compound	RLM Oxidation	GPLM Oxidation	HLM Oxidation	hCYP3A4 Oxidation
CA–DADLE	Tyr^1, Phe^4	Tyr^1, Phe^4	Tyr^1	Phe^4
CA–[Cha^4,D-Leu^5]–Enk	Tyr^1	Tyr^1, Cha^4	Tyr^1, Cha^4	No significant metabolites
CA–[Cha^4,D-Ala^5]–Enk	Tyr^1	Tyr^1	Tyr^1	No significant metabolites

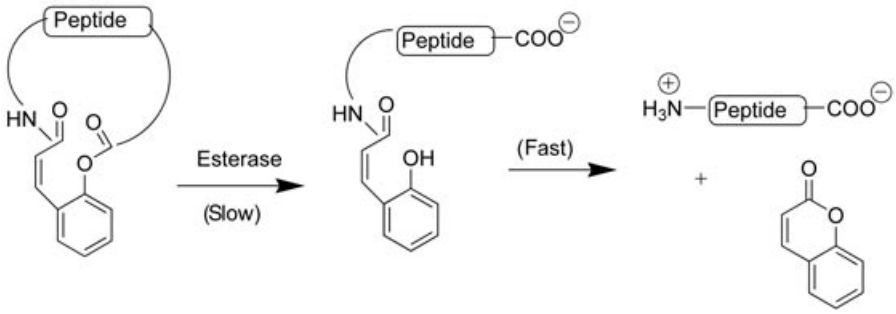

Figure 10. Scheme for the bioconversion of the ester-based cyclic prodrugs.

change as well as an additional modification at the fifth amino acid residue (e.g., Leu^5 to Ala^5), creating CA–[Cha^4,D-Ala^5]–Enk (**3**; Fig. 1). The rationale for this change in the fifth amino acid from D-Leu^5 to D-Ala^5 was to hopefully increase the rate of bioconversion of the prodrug by esterases (Fig. 10). Cleavage of the ester bond formed between the carboxylic acid of the fifth amino acid and the phenolic group of the coumarin linker results in the formation of a linear intermediate (Fig. 10). This intermediate then undergoes intramolecular lactonization, resulting in the formation of coumarin and the linear peptide. Because hydrolysis of the ester bond is the rate-determining step in the bioconversion, a rapid rate of hydrolysis of this bond would be preferred. The presences of D-Ala as the fifth amino acid in CA–[Cha^4,D-Ala^5]–Enk provides reduced steric bulk around the ester bond, leaving it more exposed to esterases and potentially aiding in the bioconversion of the cyclic prodrug. In support of this idea, it has been shown that a decrease in steric bulk around the ester bond increases the lactonization rate in similar cyclic prodrugs.[41] The D-enantiomer of Ala instead of the L-enantiomer was used in this analog because in the enkephalin class of opioid peptides, the chirality of this amino acid has been shown to greatly affect the opioid peptide's stability toward peptidases.[10,11]

The strategy for the synthesis of the two CA–DADLE analogs was taken from a retrosynthetic analysis of the structures of the desired molecules. Retrosynthetically, the bond between the fourth and fifth amino acid was broken, leading to a linear precursor (Fig. 2). The molecule was then further broken down into two parts: (i) a tetrapeptide arm and (ii) a linker moiety containing the fifth amino acid. These two parts were the building blocks for the convergent synthesis of the cyclic peptide prodrug analogs. The advantage of using this method is that all the cyclic prodrugs can be constructed from these building blocks. Thus, this strategy provides a reduction in the amount of synthetic work required to make the desired cyclic prodrugs.

In Vitro Microsomal Stability

The metabolic stability and metabolite identification studies of CA–DADLE, CA–[Cha^4,D-Leu^5]–Enk, and CA–[Cha^4,D-Ala^5]–Enk were performed in the presence of animal and HLM (e.g., RLM, GPLM, and HLM). All of the cyclic prodrugs were found to be very unstable in the presence of animal and human microsomes (Figs. 5–7). In contrast, DADLE was found to be metabolically stable in these microsomal preparations.

The instabilities of cyclic prodrugs **1**–**3** in these microsomal preparations were shown to arise from oxidative metabolism mediated by CYP450 enzymes. For example, the stability of CA–DADLE and CA–[Cha^4,D-Ala^5]–Enk could be increased fourfold when ketoconazole, a CYP450 inhibitor, was included in the incubation media. For CA–[Cha^4,D-Leu^5]–Enk, the results are less dramatic, showing only a twofold increase. Overall, these results suggest that CA–[Cha^4,D-Leu^5]–Enk is slightly more stable toward CYP450-mediated oxidative metabolism than cyclic prodrugs **1** and **3**. Also, although the addition of ketoconazole results in a significant increase in the amount of cyclic prodrugs recovered, the addition of paraoxon, an esterase B inhibitor, only marginally increased the amount of cyclic prodrugs recovered from the incubation media (Figs. 5–7). This suggests that the metabolic instability of cyclic prodrugs **1**–**3** does not arise from premature bioconversion of the ester prodrugs.

Interestingly, when metabolic stability assays are performed in the presence of hCYP3A4, very different results were observed. Although CA–DADLE was found to be metabolically unstable in the presence of hCYP3A4, the CA–DADLE analogs **2** and **3** were found to be quite stable under the same experimental conditions (Fig. 8). CA–[Cha^4,D-Leu^5]–Enk and CA–[Cha^4,D-Ala^5]–Enk both showed more than 75% cyclic prodrug recovered in the presence of hCYP3A4 without inhibitors as compared with 9% recovered for CA–DADLE (Fig. 8). With the addition of

ketoconazole, the recovery of cyclic prodrugs **2** and **3** increased to more than 95%. These results indicate that CA–[Cha^4,D-Leu^5]–Enk and CA–[Cha^4,D-Ala^5]–Enk are not metabolized by hCYP3A4 to the same extent as CA–DADLE. However, when these results using recombinant hCYP3A4 are compared with the animal and human microsomal stability data described above, one must conclude that CA–[Cha^4,D-Leu^5]–Enk and CA–[Cha^4,D-Ala^5]–Enk are good substrates for other CYP450 isozymes.

The stability of the CA moiety to oxidative metabolism reveals that the addition of this chemical moiety is not directly responsible for the metabolic instability of the cyclic prodrugs **1**–**3**. Also having shown separately that DADLE is stable to oxidative metabolism leads to the conclusion that the physiochemical properties (e.g., increased lipophilicity) and/or the increased rigidity of the cyclic produgs is responsible for the metabolic instability of the cyclic prodrugs **1**–**3**. By restricting the solution conformation of the peptide portion of these prodrugs, amino acid side chains (e.g., Phe^4) must assume conformations that facilitate their binding to CYP450 isozymes and their subsequent conversion to oxidative metabolites. In addition, it is not unexpected to observe what appear to be differences in substrate activity of these cyclic prodrugs for different CYP450 isozymes. It is interesting to note that opioid peptides themselves have been shown to have a diminished binding affinity to their receptor upon cyclization, which is hypothesized to arise from the decreased flexibility of the cyclic compounds.[26–28]

Metabolite Identification

Metabolite identification studies were performed in order to identify the specific sites of oxidative metabolism on the cyclic prodrugs **1**–**3**. The primary sites of oxidation were at Phe/Cha^4 and Tyr^1. Because the opioid activity of peptides and peptidomimetics has been shown to be highly dependent on an unmodified Tyr^1 on the peptide chain,[31,37,34,35] it was decided not to modify this amino acid in an attempt to improve its metabolic stability. This decision was made in spite of the fact that the oxidation on Tyr^1 gives rise to the majority of the metabolites for all three cyclic prodrugs (Table 1). In the presence of microsomes, cyclic prodrug **3** shows fewer oxidative metabolites than CA–DADLE. However, analog **3** did not show better metabolic stability in the microsomal assays as compared with CA–DADLE (Figs. 5–7). The reason for the similarities in the extent of oxidative metabolism of cyclic prodrugs **1** and **3** could arise from the change of Phe^4 to Cha^4 in **3**, making Tyr^1 more susceptible to hydroxylation in the presence of liver microsomes.

The metabolite identification results are very different in the presence of hCYP3A4 than in the liver microsomal assays. After a 60 min incubation with hCYP3A4, CA–DADLE showed hydroxylation at Tyr^1, whereas the cyclic prodrugs **2** and **3** showed no significant metabolite formation (Table 1). This is consistent with the metabolic stability results, which showed cyclic prodrugs **2** and **3** to have greatly enhanced metabolic stability in the presence of hCYP3A4 (Fig. 8). Because CYP3A4 is an important barrier to intestinal absorption, proving that CA–[Cha^4,D-Leu^5]–Enk and CA–[Cha^4,D-Ala^5]–Enk are metabolically stable, showing no metabolite formation in the presence of hCYP3A4, is a significant result. The increased metabolic stability of the chemically modified prodrugs **2** and **3** in the presence of hCYP3A4 makes them good candidates for evaluation of their absorption after oral administration.

The potential oxidative metabolism of the CA in cyclic prodrugs **1**–**3** was carefully monitored in our metabolic stability studies. Oxidation at the site of the CA is considered a high probability because of the known metabolic susceptibility of coumarin.[42–44] Metabolite identification studies of the cyclic prodrugs **1**–**3**, however, provided no evidence for the formation of hydroxy-coumarin. In fact, the detection of unhydroxylated coumarin from the cyclic prodrugs **1**–**3** after incubation with animal and human microsomes confirmed the metabolic stability of the CA moiety in these molecules.

It should be noted that in-depth investigations into the exact structures of the oxidative metabolites formed from cyclic prodrugs **1**–**3** were not undertaken in these studies. Instead, the focus of this research was to identify the amino acids that are the sites of oxidative metabolism in these cyclic prodrugs and to use this information to design cyclic prodrug analogs that are more metabolically stable to CYP450.

CONCLUSION

The primary objective of the research described in this paper was to improve the biopharmaceutical properties, particularly metabolic stability, of a cyclic prodrug (CA–DADLE) of the opioid peptide DADLE, which had been previously synthesized in our laboratory.[17] To this end, we have designed and synthesized two new analogs of CA–DADLE and characterized their stability to oxidative metabolism mediated by CYP450 enzymes. The synthesis of these analogs involved a convergent method where a linker moiety was combined with a peptide arm and then cyclized in a final step, yielding the cyclic prodrugs **2** and **3**. The design of these analogs of CA–DADLE was based on literature knowledge about the structural requirements for the binding of opioid peptides to their pharmacological receptor and knowledge generated in studies about the oxidative metabolism of CA–DADLE. On the basis of the knowledge that Phe^4

on CA–DADLE was one of two major sites of oxidative metabolism, CA–[Cha^4,D-Leu^5]–Enk (**2**) and CA–[Cha^4,D-Ala^5]–Enk (**3**) were designed and synthesized. When incubated with animal and human microsomes, cyclic prodrug analogs **2** and **3** did not show increases in metabolic stability as compared with CA—DADLE. This finding was not totally unexpected because the second major site of oxidative metabolism (Tyr^1) on CA–DADLE was still present in analogs **2** and **3**. In the design of prodrug analogs **2** and **3**, we decided not to alter the structure of Tyr^1 because of its critical nature for pharmacological activity.[31,37,34,35] However, surprisingly, it was found that cyclic prodrug analogs **2** and **3** were significantly more stable than CA–DADLE when incubated with hCYP3A4. These results suggest that other CYP450 isozymes may be responsible for the oxidative metabolism of cyclic prodrugs analogs **2** and **3**, which was observed when the compounds were incubated with animal and HLM. The improved metabolic stability of analogs **2** and **3** toward hCYP3A4 may, however, be very important from an oral absorption perspective because this CYP450 isozyme is highly expressed in intestinal mucosal cells and is known to limit the oral bioavailability of some drugs.[45–50]

ACKNOWLEDGMENTS

The authors would like to thank Dr. Teruna Siahaan for his helpful discussion and insight into the synthetic strategy. This research was made possible by the financial support of National Institute of General Medical Sciences Predoctoral Biotechnology Training Grant and a research grant from National Institute on Drug Abuse (DA-03315).

REFERENCES

1. Gentilucci L. 2004. New trends in the development of opioid peptide analogs as advanced remedies for pain relief. Curr Top Med Chem 4:19–38.
2. Knipp GT, Vander Velde DG, Siahaan TJ, Borchardt RT. 1997. The effect of β-turn structure on the passive diffusion of peptides across Caco-2 cell monolayers. Pharm Res 14:1332–1340.
3. Schiller PW. 1993. Development of receptor-selective opioid peptide analogs as pharmacological tools and as potential drugs. Handb Exp Pharmacol 681–710.
4. Schiller PW. 2005. Opioid peptide-derived analgesics. AAPS J 7(3):E560–E565.
5. Witt KA, Davis TP. 2006. CNS drug delivery; opioid peptides and the blood–brain barrier. AAPS J 8(1):E76–E88.
6. Borchardt RT. 1999. Optimizing oral absorption of peptides using prodrug strategies. J Control Release 62:231–238.
7. Han C, Liu S, Wang B. 2002. Major factors influencing peptide drug absorption. Front Biotechnol Pharm 3:270–290.
8. Wang W, Camenisch G, Sane DC, Zhang H, Hugger E, Wheeler GL, Borchardt RT, Wang B. 2000. A courmarin-based prodrug strategy to improve the oral absorption of RGD peptidomimetics. J Control Release 65:245–251.
9. Yang JZ, Chen W, Borchardt RT. 2002. *in vitro* stability and *in vivo* pharmacokinetic studies of a model opioid peptide, H-Tyr–D-Ala–Gly–Phe–D-Leu–OH (DADLE), and its cyclic prodrugs. J Pharmacol Exp Ther 303(2):840–848.
10. Beddell CR, Clark RB, Lowe LA, Wilkinson S, Chang KJ, Cuatrecasas P, Miller R. 1977. A conformational analysis for leucine–enkephaline using activity and binding data of synthetic analogues. Br J Pharmacol 61:351–356.
11. Belluzzi JD, Stein L, Dvonch W, Dheer S, Gluckman MI, McGregor WH. 1978. Enhanced analgesic activity of D-Ala^2 enkephalinamides following D-isomer substitutions at position five. Life Sci 23(2):99–104.
12. Ouyang H, Tang F, Siahaan TJ, Borchardt RT. 2002. A modified coumarinic acid-based cyclic prodrug of an opioid peptide: Its enzymatic and chemical stability and cell permeation characteristics. Pharm Res 19(6):794–801.
13. Tang F, Borchardt RT. 2002. Characterization of the efflux transporter(s) responsible for restricting intestinal mucosa permeation of the coumarinic acid-based cyclic prodrug of the opioid peptide DADLE. Pharm Res 19(6):787–793.
14. Chen W, Yang JZ, Andersen R, Nielsen LH, Borchardt RT. 2002. Evaluation of the permeation characteristics of a model opioid peptide, H-Tyr–D-Ala–Gly–Phe–D-Leu–OH (DADLE), and its cyclic prodrugs across the blood–brain barrier using an *in situ* perfused rat brain model. J Pharmacol Exp Ther 303:849–857.
15. Ouyang H, Anderson TE, Chen W, Nofsinger R, Steffansen B, Borchardt RT. 2009. A comparison of the effects of P-glycoprotein inhibitors on the blood–brain barrier permeation of cyclic prodrugs of an opioid peptide (DADLE). J Pharm Sci 98:2227–2236.
16. Uchiyama T, Kotani A, Tatsumi H, Kishida T, Okamoto A, Okada N, Murakami M, Fujita T, Fujiwara Y, Kiso Y, Muranishi S, Yamamoto A. 2000. Development of novel lipophilic derivatives of DADLE (leucine enkephalin analog): Intestinal permeability characteristics of DADLE derivatives in rats. Pharm Res 17:1461–1467.
17. Ouyang H, Borchardt RT, Siahaan TJ, Vander Velde DG. 2002. Synthesis and conformational analysis of a coumarinic acid-based cyclic prodrug of an opioid peptide with modified sensitivity to esterase-catalyzed bioconversion. J Pept Res 59(4):183–195.
18. Gudmundsson OS, Jois SDS, Velde DGV, Siahaan TJ, Borchardt RT, Wang B. 1999. The effect of conformation on the membrane permeation of coumarinic acid and phenylpropionic acid based cyclic prodrugs of opioid peptides. J Pept Res 53:383–392.
19. Wang B, Nimkar K, Wang W, Zhang H, Shan D, Gudmundsson O, Gangwar S, Siahaan T, Borchardt RT. 1999. Synthesis and evaluation of the physicochemical properties of esterase sensitive cyclic prodrugs of opioid peptides using coumarinic acid and phenylpropionic acid linkers. J Pept Res 53(4):370–382.
20. Ouyang H, Chen W, Anderson TE, Steffansen B, Borchardt RT. 2009. Factors that restrict intestinal cell permeation of cyclic prodrugs of an opioid peptide (DADLE): Part I. Role of efflux transporters in the intestinal mucosa. J Pharm Sci 98:337–348.
21. Ouyang H, Chen W, Anderson TE, Steffansen B, Borchardt RT. 2009. Factors that restrict intestinal cell permeation of cyclic prodrugs of an opioid peptide (DADLE): Part II. Role of metabolic enzymes in the intestinal mucosa. J Pharm Sci 98:349–361.
22. Bak A, Gudmundsson OS, Friis GJ, Siahaan TJ, Borchardt RT. 1999. (Acyloxy)alkoxy-based cyclic prodrugs of opioid peptides: Evaluation of the chemical and enzymatic stability as well as their transport properties across Caco-2 cell monolayers. Pharm Res 16:24–29.
23. Gudmundsson OS, Nimkar K, Gangwar S, Siahaan T, Borchardt RT. 1999. Phenylpropionic acid-based cyclic

prodrugs of opioid peptides that exhibit metabolic stability to peptidases and excellent cellular permeation. Pharm Res 16:16–23.
24. Gudmundsson OS, Pauletti GM, Wang W, Shan D, Zhang H, Wang B, Borchardt RT. 1999. Coumarinic acid-based cyclic prodrugs of opioid peptides that exhibit metabolic stability to peptidases and excellent cellular permeability. Pharm Res 16:7–15.
25. Tang F, Borchardt RT. 2002. Characterization of the efflux transporter(s) responsible for restricting intestinal mucosa permeation of an acyloxyalkoxy-based cyclic prodrug of the opioid peptide DADLE. Pharm Res 19(6):780–786.
26. Patel J, Mitra AK. 2001. Strategies to overcome simultaneous P-glycoprotein-mediated efflux and CYP3A4-mediated metabolism of drugs. Pharmacogenomics 2:401–415.
27. Wacher VJ, Silverman JA, Zhang Y, Benet LZ. 1998. Role of P-glycoprotein and cytochrome P450-3A in limiting oral absorption of peptides and peptidomimetics. J Pharm Sci 87:1322–1330.
28. Wang Ej, Lew K, Barecki M, Casciano CN, Clement RP, Johnson WW. 2001. Quantitative distinctions of active molecular recognition by P-glycoprotein and cytochrome P450 3A4. Chem Res Toxicol 14:1596–1603.
29. Zhang Y, Guo Z, Lin ET, Benet LZ 1998. Overlapping substrate specificties of cytochrome P450-3A and P-glycoprotein for a novel cysteine protease inhibitor. Drug Metab Dispos 26:360–366.
30. Filippi B, Giusti P, Cima L, Borin G, Ricchelli F, Marchiori F. 1979. Addicting properties and conformational studies in solution. Int J Pept Protein Res 14:34–40.
31. Hruby VJ, Bartosz-Bechowski H, Davis D, Slaninova J, Zalewska T, Stropova D, Porreca F, Yamamura HI. 1997. Cyclic enkephalin analogues with exceptional potency and selectivity for δ-opioid receptors. J Med Chem 40:3957–3962.
32. Lazarus LH, Salvador S, Balvoni G, Tomatis R, Wilson WE. 1992. Stereospecificity of amino acid side chains in deltorphin defines binding to opioid receptors. J Med Chem 35:1222–1227.
33. McFadyen IJ, Sobczyk-Kojiro K, Schaefer MJ, Ho JC, Omnaas JR, Mosberg HI, Traynor JR. 2000. Tetrapeptide derivatives of [D-Pen^2, D-Pen^5]–enkephalin (DPDPE) lacking an N-terminal tyrosine residue are agonists at the opioid receptor. J Pharmacol Exp Ther 295:960–966.
34. Morgan BA, Smith CFC, Waterfield AA, Huges J, Kosterlitz HW. 1976. Structure–activity relationships of methionine–enkephalin. J Pharm Pharmacol 28:660–661.
35. Schmidt R, Menard D, Mrestani-Klaus C, Chung NN, Lemieux C, Schiller PW. 1997. Structural modifications of the N-terminal tetrapeptide segments of [D-Ala2]-deltrophin I: Effects on opioid receptor affinities and activities *in vitro* and on antinociceptive potency. Peptides 18:1615–1621.
36. Liederer BM, Phan KT, Ouyang H, Borchardt RT. 2005. Significant differences in the disposition of cyclic prodrugs of opioid peptides in rats and guinea pigs following IV administration. J Pharm Sci 94:2676–2687.
37. Lazarus L, Salvador S, Balvoni G, Tomatis R, Wilson W. 1992. Stereospecificity of amino acid side chains in deltorphin defined binding to opioid receptors. J Med Chem 35:1222–1227.
38. Becker JA, Wallace A, Garzon A, Ingallinella P, Bianchi E, Cortese R, Simonin F, Kieffer BL, Pessi A. 1999. Ligands for K-opioid and ORL1 receptors identified from a conformationally constrained peptide combinatorial library. J Biol Chem 274:27513–27522.
39. Weltrowska G, Lemieux C, Chung NN, Schiller PW. 2004. A chimeric opioid peptide with mixed mu agonist/gamma antagonist properties. J Pept Res 63:63–68.
40. Toth G, Ioja E, Tomboly C, Ballet S, Tourwe D, Peter A, Martinek T, Chung NN, Schiller PW, Benyhe S, Borsodi A. 2007. Beta-methyl substitution of cyclohexylalanine in Dmt–Tic–Cha–Phe peptides results in highly potent gamma opioid antagonist. J Med Chem 50:328–333.
41. Zaych LA, Yang W, Liao Y, Griffin KR, Wang B. 2004. The effect of substitution patterns on the release rates of opioid peptides DADLE and [Leu^5]–enkephalin from coumarin prodrug moieties. Bioorg Chem 32:109–123.
42. Lewis DFV, Ito Y, Lake BG. 2006. Metabolism of coumarin by human P450's: A molecular modeling study. Toxicol In Vitro 20:256–264.
43. Mead JA, Smith JN, Williams RT. 1958. Studies in detoxication.72. The metabolism of coumarin and of o-coumarinc acid. Biochem J 68:67–74.
44. Mead JA, Smith JN, Williams RT. 1958. Studies in detoxication.71. The metabolism of hydroxycoumarins. Biochem J 68:61–67.
45. Bailey DG, Malcolm J, Arnold O, Speuce J. 1998. Grapefruit juice drug interactions. Br J Clin Pharmacol 46:101–110.
46. Hebert MF. 1997. Contributions of hepatic and intestinal metabolism and P-glycoprotein to cyclosporine and tacrolimus oral drug delivery. Adv Drug Deliv Rev 27:201–214.
47. Kolars JC, Schmiedlin-Ren P, Scheutz JD, Fang C, Watkins PB. 1992. Identification of rifampin-inducible P450IIIA4 (CYP3A4) in human small bowl enterocytes. J Clin Invest 90:1871–1878.
48. Obach SR, Zhang QY, Dunbar D, Kaminsky LS. 2001. Metabolic characterization of the major human small intestinal cytochrome P450s. Drug Metab Dispos 29:347–352.
49. Watkins PB. 1997. The barrier function of CYP3A4 and P-glycoprotein in the small bowel. Adv Drug Deliv Rev 27:161–170.
50. Zhou SF. 2008. Drugs that behave as substrates, inhibitors and inducers of human cytochrome P4503A4. Curr Drug Metab 9:310–322.